



ORIGINAL ARTICLE

Optical properties and aggregation behavior of environmentally friendly Lanthanum (III) acyl–alaninate complexes

Gerile Naren^{a,b,*}, Tana Bao^a, Jun Ning^{a,b}, O. Tegus^{a,b}

^a College of Physics and Electronic Information, Inner Mongolia Normal University, Hohhot 010022, China

^b Inner Mongolia Key Laboratory for Physics and Chemistry of Functional Materials, Inner Mongolia Normal University, Hohhot 010022, China

Received 28 January 2020; accepted 18 April 2020

Available online 27 April 2020

KEYWORDS

Rare earth organic complex;
Aggregation behavior;
Surfactant;
Liquid state;
Glassy state

Abstract Rare earth organic complex materials have attracted tremendous attention for their intrinsic properties and promising practical applications. It is still a great challenge to realize the rare earth organic complex materials with excellent functional properties and diversified structural states. Here, the amino acid rare earth surfactant complexes of lanthanum octanoyl-alaninate (La(oct-ala)₃), lanthanum octanoyl-serinate (La(ser-oct)₃) and lanthanum octanoyl-phenylalaninate (La(oct-phe)₃) were synthesized by the reaction of C₁₁H₂₁NO₃, C₁₁H₂₁NO₄, C₁₇H₂₆NO₃ with LaCl₃, respectively. As-synthesized complexes of La(oct-ala)₃ and La(oct-phe)₃ have high solubility in pure solvent, while the solubility of La(ser-oct)₃ is very low in pure solvent. When the concentration of the complex solution is lower than the critical micelle concentration, the dissociation phenomenon of the complex is occurred in the solution. When the concentration of the complex solution is greater than the critical micelle concentration, the dissociated ligand ions and metal ions will associate, which can form micelle aggregates. In addition, the aggregates of the complex gradually shrink to form aggregates of different sizes and sizes as the solvent continues to volatilize. By further heating and cooling, the glassy, crystalline, liquid crystal and other complexes can be obtained. The rare earth organic low molecular complexes formed by the combination of these rare earth ions and amino acid ligands can not only obtain the complexes with high rare earth content, but also have the excellent properties of convenient synthesis, high yield, easy processing, good solubility, low toxicity and high stability, etc., which can play the special physical and chemical functional characteristics of the diversified structure state of rare earth organic molecular materials. Therefore,

* Corresponding author.

E-mail address: naren88@hotmail.com (G. Naren).

Peer review under responsibility of King Saud University.



Production and hosting by Elsevier

in present work, the lanthanum complexes as a functional molecular materials have potential applications in many fields.

© 2020 The Authors. Published by Elsevier B.V. on behalf of King Saud University. This is an open access article under the CC BY license (<http://creativecommons.org/licenses/by/4.0/>).

1. Introduction

Amphoteric metal soap salts, such as metal salts of fatty acids, play an important role in daily life. At room temperature, many of the amphoteric metal soap salts have very low solubility and difficult to solve in pure solvents and water/organic solvent mixtures. Thus, it is difficult for them to gather to form micelles. Furthermore, if micelles are formed, the ability of micelles to adsorb water is less (Kadoda, 2006). The common metal elements in soaps include calcium, magnesium, zinc, lead, aluminum, manganese, iron, cobalt, nickel, molybdenum, barium, cadmium, etc (Kadoda, 2006). Most of the metal soaps are not soluble in water and in ethanol. Some of the metal soaps can be dissolved in turpentine or solvent gasoline; some can be dispersed in organic solvents. Organometallic soaps are one of the common lubricants, or polyvinyl chloride (PVC) heat stabilizers. The solubility of the soaps in water and organic solution is low, which limits significantly the application of amphoteric metallic soap. Research work mainly focuses on the solubility of the metal soap in solvents and its aggregation behavior in solution at high temperatures (about 100 °C) (Kadoda, 2006; Jiao et al., 2009; Iida, 2002; Iida et al., 2004; Iida et al., 2006; Naren et al., 2008; Naren et al., 2009).

In recent years, the octanoyl alanine amino acid series of metal complexes (such as $\text{Mg}(\text{oct-ala})_2$ and $\text{Ca}(\text{oct-ala})_2$) received an extensive attention due to the indication of their unique structural diversity (such as amorphous, glassy state, liquid state), ecological and environmental advantages being beneficial to human health. In addition, the preparation process and use of these new types of organic substrate materials are also intensively investigated (Iida et al., 2004; Iida et al., 2006; Gerile et al., 2015). The molecular crystal of metal complex is formed from neutral molecule, with the center of gravity of the molecule oriented and ordered at low temperature; it usually leads to optical anisotropy. Besides, molecular glasses of these metal complexes have excellent flexibility, transparency, uniformity and isotropic properties. The formation of a thermodynamic non-equilibrium glass state after freezing molecular motion is a widely used concept in modern materials science (Wang et al., 2011; Szwarc and Bessada, 1995). But, examples of studies are scarce on metal complexes at the molecular level of sol, gel and glassy states of the alkyl chain of metal complexes.

As the appropriate hydrophilic hydrophobic balance alkyl chain metal complexes have high solubility and aggregation behavior in organic solvent rally, the high solubility and aggregation behavior of these complexes affect the diverse structural properties of the metal complex. Therefore, the high aggregation phenomenon of the hydrophilic and hydrophobic equilibrium of the metal complexes in this paper is the basis, with the ligands carrying the hydrophobic groups and carrying the hydrophilic groups selected and prepared. Phenylalan bulky hydrophobic octanoylalanine (=H(oct-phe)) or serin bulky hydrophilic octanoylserine (=H(oct-ser)) objects are introduced to replace the original alanine ligand. Hereafter, the metal complexes were synthesized and separated, with the physical and chemical properties of these compounds further studied.

Previously, researchers reported that the high stability of liquid crystal glass is usually formed in the liquid crystal polymer, as a high performance material applied in many research fields (Seiji and Hirosh, 2014). However, liquid crystal polymers have high viscosity, and in many cases it is difficult to precisely control the molecular arrangement. On the contrary, $\text{La}(\text{oct-ser})_3$ complex, which is a newly synthesized low molecular weight rare earth compound, has an orientation control. The orientation of liquid crystal field coordination in solid

state can be maintained easily to form low molecular liquid crystal glass, and can replace the original liquid crystal materials, looking forward to generating molecular glass materials in many areas of application development. In the X-ray diffraction measurement, a sharp reflection in a small corner shows that the layer structure of the smectic phase is retained even in the solid phase when the complex appears, and that these materials do not exhibit any characteristic crystallization peak. We believe that the formation of this clear liquid crystal glass is due to the Coulomb interaction between anions and cations acting over long distances.

Coordination compounds, including Metal-organic frameworks (MOFs) have well-defined pore structures and promising properties (Yusuf et al., 2017; Azhar et al., 2019; Tang et al., 2016; Kaneti et al., 2017), are emerging molecular solids with promising properties, as a precursor for preparing porous hybrid materials, it has attracted extensive attention. We believe that the rapid development of these lanthanum complexes in this field can be expected.

Related studies showed that such complexes had small pollution towards ecology and the environment, and it was beneficial to a variety of areas, such as organic light emitting diodes, organic solar cells, single molecular magnets, rare earth luminescent materials, etc. (Li et al., 2016; Li et al., 2017; Zhang, 2017), indicating that the new complexes we synthesized are promising new green environment materials (Iida, 2002; Iida et al., 2004; Iida et al., 2006; Naren et al., 2008; Naren et al., 2009; Gerile et al., 2015; Li et al., 2017; Zhang, 2017; Naren et al., 2016; Hua et al., 2011; Du et al., 2003).

2. Experimental

2.1. Materials

The raw material reagents used for synthesizing the metal complexes of amino acids with different polar groups and the standard reagents used for the measurement experiments are listed: DL- α -alanine (Wako Pure pharmaceutical), DL-phenylalanine (Wako Pure pharmaceutical), L-serine (Wako Pure pharmaceutical), Octanoyl chloride (Tokyo Chemical), and Lanthanum chloride (Wako Pure pharmaceutical). Methanol and ethanol were distilled, and the water used in this study was subjected to secondary distillation. The deuterated solvent (methanol d_4 (=MeOD)) for NMR measurements was provided by Merck Co.

2.2. Preparation methods

Ligands and the metal complexes were prepared following previous reports (Naren et al., 2008; Naren et al., 2009; Zhang, 2017). N-octanoyl-dl-alanine (=oct-ala), N-octanoylserine (=ser-act), and N-octanoyl-dlphenylalanine (=oct-phe) were obtained by the reported procedures (Naren et al., 2008; Naren et al., 2009). The bis(N-octanoylalaninato) ($\text{La}(\text{oct-ala})_3$), bis(N-octanoylphenylalaninato) ($\text{La}(\text{oct-phe})_3$), and N-octanoylserinenato (=La(ser-act) $_3$) complexes were prepared by reactions of Lanthanum chloride ($1.1 \times 10.2 \text{ mol}$) with the corresponding acylamino acids ($3 \times 10.2 \text{ mol}$) in distilled methanol. The obtained complexes were subjected to

recrystallization treatment using a mixed solution of acetone and methanol. The elemental analyses of C, H, and N were performed using Perkin-Elmer model 2400II. Water content of the complexes are determined by Karl-Fisher titration. The purity of the complexes were determined by ^{13}C NMR spectroscopy. The molecular structure of the complex is shown in Fig. 1.

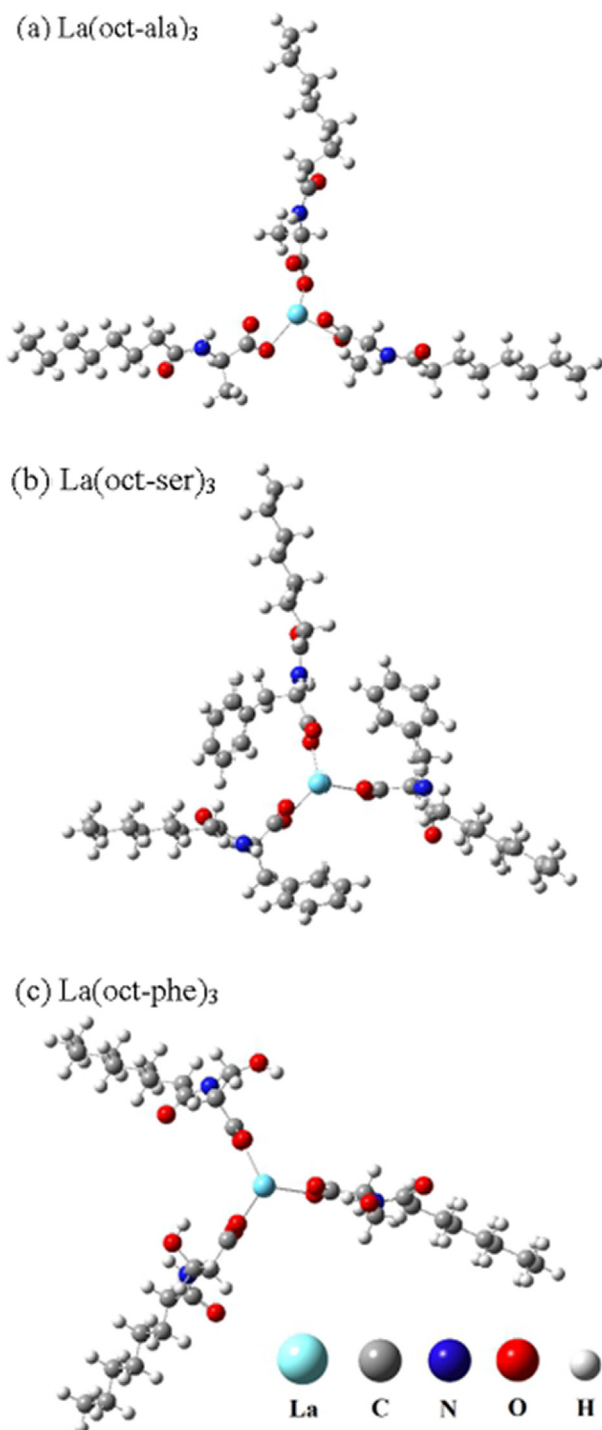


Fig.1 (a) $\text{La}(\text{oct-ala})_3$, (b) $\text{La}(\text{oct-ser})_3$, (c) $\text{La}(\text{oct-phe})_3$ complex.

2.3. Measurements

2.3.1. NMR measurements

The ^{13}C NMR spectra in La complex solution were measured using a JEOL EX-270 FT NMR spectrometer operating at 67.9 MHz. ^1H NMR self-diffusion coefficient was measured without rotating the sample at a measuring frequency of 90 MHz and a temperature of 27 °C. The measurements were performed with a JOEL Mac FX-90 spectrometer. In order to see the self-association behavior of these complexes in solution, the self-diffusion coefficient D of the amino acid metal complex surfactant and of the solvent was measured by Pulsed Field Gradient Spin Echo (PGSE) (Naren et al., 2008; Naren et al., 2009; Du et al., 2003).

2.3.2. Vapor pressure depression measurements

The association behavior of these La complexes in methanol solutions were studied using a Knauer vapor pressure Osmometer (VPO) at 45 °C. VPO provides the apparent molecular weight of the complexes. Methods of measurement were based on our previous reports (Naren et al., 2008; Mizuno et al., 1998). For Knauer vapor pressure Osmometer measurements, a temperature difference ($T-T_0$) between a solution, in which a low molecular weight compound having a known molecular weight is a solute (Benzyl for methanol solution), and a pure solvent is measured. The apparent molecular weight of the lanthanide complexes were obtained through the relationship between T and the concentration of the solute.

2.3.3. Electric conductivities

The dissociation of the octanoyl amino acid ligand from the La complexes in methanol solution was detected by HORIBA B 173 conductivity meter. The electrical conductivity (κ (mS cm^{-1})) was measured using a 0.01 mol dm^{-3} KCl aqueous solution at 25 ± 1 °C ($\kappa = 1.41 \text{mS cm}^{-1}$) as the standard. The conductivity of a sample with a volume of less than 5 cm^3 can be measured.

2.3.4. Polarizing optical micrographs

The surface morphology of the rare earth complexes was observed using LABOPHOT-POL Nikon polarized light microscope. The same specimens were used for the DSC measurements. The glass state material shows isotropic optical properties, while the crystal and liquid crystal materials show the anisotropic optical properties.

2.3.5. Calorimetric measurements

The Characterization of the solid state and loss of water from the solids were followed by DSC (with a Shimadzu DSC-50), TG-DTA (with a Rigaku TG8101 or with a Shimadzu DTG-60) in the temperature range 20–250 °C. The samples (3–5 mg) were placed in aluminum pans and run at a rate of 10 K min^{-1} under nitrogen gas at a flow rate of 15 mL min^{-1} . Indium metal was used as standard for temperature and enthalpy calibrations.

2.3.6. X-ray measurements

X - ray diffraction measurements were carried out in order to determine the crystalline state and liquid crystal state of the complex. Wide-angle ($2\theta = 5\text{--}60^\circ$) X-ray diffractions

(WAXD) and small-angle ($2\theta = 1\text{--}10^\circ$) X-ray scatterings (SAXS) were measured at room temperature with a 0.8 KW generator of Cu K α radiation (PANalytical X'pert Pro) and with a 1.6 KW generator of Cu K α radiation (Rigaku RINT-Ultima III), respectively.

2.3.7. FT-IR measurements

The FT-IR spectra were measured in the range 400–4000 cm^{-1} on a SHIMADZU 8300 spectrometer by the KBr pellet method for the glassy, crystalline and liquid crystalline specimens. Firstly, after measuring the background, next the main measurement was carried out. The average of the results obtained by several measured results and the irregular occurrence of the simulated absorption results, a good spectrum has been obtained from a small sample test. For all samples, the number of integrations was 24. In particular, the antisymmetric stretching band of the methylene chain around 2850–2960 cm^{-1} was qualitatively analyzed.

2.3.8. EXAFS measurements

Extended X-ray absorption fine structure (EXAFS) measurements at the La L $_3$ -edge (5484.0 eV) were performed at room temperature in transmission mode at the BL-7C station of the photon Factory, High Energy Accelerator Research Organization in Japan (KEK-PF). The ring current was 300–450 mA, and the storage ring was operated with an electron energy of 2.5 GeV. A reference compound (La(acac) $_2$ (H $_2$ O) $_2$ solid) was used to evaluate the validity of the theoretical phase shift and back-scattering amplitude functions proposed by Mckale, et al (Silverstein et al., 2014).

3. Results and discussion

3.1. Elemental (CHN) analysis

Crystalline and glass solids are isolated by the following method. After the evaporation of the reaction solvent, the La(oct-ala) $_3$ complex forms a crystalline-amorphous mixture (the appearance is a white powder), and heated at 110 $^\circ\text{C}$ for 2 h and rapidly cooled to form monohydrate isotropic stable glass state complexes. When a small amount of water is added from the concentrated methanol solution and the La complexes is separated, an anisotropic stable crystalline monohydrate complex is formed. The acetone has been added to methanol solution, to form monohydrate isotropic stable glass state complexes (Hua et al., 2011). After the evaporation of the reaction solvent, the La(oct-phe) $_3$ complex forms a 1.5 hydrate White crystalline material, and heated at 110 $^\circ\text{C}$ for 2 h and

rapidly cooled to form 1.5 hydrate An anisotropic stable liquid crystalline state complex is formed (Hua et al., 2011). La(oct-ser) $_3$ complexes were obtained by evaporation of solvent methanol and vacuum drying to obtain optically anisotropic 3 water complexes, the complexes were appear glass transition point in the DSC test. The above test results show that the formation of a new Aggregation substance state solid. Likewise, the complex was heated at 110 $^\circ\text{C}$ for 2 h and rapidly cooled. However, this complex still retains the original water content and anisotropic properties, and does not form isotropic glassy matter.

The elemental (CHN) analyses were performed using Perkin-Elmer model 2400II. For La(oct-ala) $_3$ glassy and La(oct-ala) $_3$ crystalline, the 1-hydrates were used for the elemental analyses; the La(oct-phe) $_3$ liquid crystalline and La(oct-phe) $_3$ crystalline, the 1.5-hydrates were used for the elemental analyses; the La(oct-ser) $_3$ liquid crystalline, the 3-hydrates were used for the elemental analyses. Table 1 shows the calculated and measured values of C, H, N elemental analysis for crystalline, liquid crystalline and glassy state Lanthanum complexes. The water content in the Complexes was examined by Karl fischer titration method. In addition, the chemical composition of the Lanthanum (III) complexes was determined using ^{13}C NMR Nuclear magnetic resonance (NMR) spectroscopy (Iida et al., 1997; Iida et al., 1998; Iida et al., 2002; Hua et al., 2003; Perju et al., 2015; Hua et al., 2007). As can be seen from Table 1, the measured and calculated values of these elements are within the allowable error range. Furthermore, the results of elemental analysis and ^{13}C NMR analysis results are consistent, and the chemical composition of the rare earth complexes can be determined to be $[\text{CH}_3(\text{CH}_2)_6\text{CONHCH(R)COO}]_3\text{La}\cdot x\text{H}_2\text{O}$ (R is CH $_3$, CH $_2$ OH, CH $_2$ C $_6$ H $_5$; x is 1, 2, 3).

3.2. Solubility in pure solvent systems of metal complexes

Table 2 shows the solubility of octanoylalanine complexes in various pure solvents at 25 ± 1 $^\circ\text{C}$. According to the reported classification (Naren et al., 2008; Naren et al., 2009), the solubility of the complex was divided into three categories: (1) more than 10% (g/mL); (2) from 0.1% (g/mL) to 10% (g/mL); and (3) less than 0.1% (g/mL). At 25 ± 1 $^\circ\text{C}$, first weigh 0.03 g of sample, add 300 μL of pure solvent, observe the solubility, if there is a dissolution phenomenon, judge it as more than 10% (w/V); if there is a non dissolution phenomenon, continue to add the solvent (each addition amount is 100 μL), judge it as 10% – 0.1% (w/V) when there is a dissolution phenomenon between 300 μL and 30 mL; If the above conditions are not solved and the amount of added solvent is

Table 1 Elemental analysis of the rare earth solid complexes.

Metal complexes	Calculated value %			Measured value %		
	C	H	N	C	H	N
La(oct-ala) $_3$ ·H $_2$ O crystalline	49.55	7.81	5.26	49.43	7.73	5.49
La(oct-ala) $_3$ ·H $_2$ O glassy	49.55	7.81	5.26	49.49	7.75	5.52
La(oct-ser) $_3$ ·3H $_2$ O liquid crystalline	44.80	7.52	4.75	44.91	7.12	4.92
La(oct-phe) $_3$ ·1.5H $_2$ O crystalline	59.06	7.25	4.05	58.86	7.14	3.89
La(oct-phe) $_3$ ·1.5H $_2$ O liquid crystalline	59.06	7.25	4.05	58.86	7.24	3.81

Table 2 Solubility (g/mL) of the lanthanum (III) octanoyl-carboxylates in various solvents at 25 ± 1 °C.

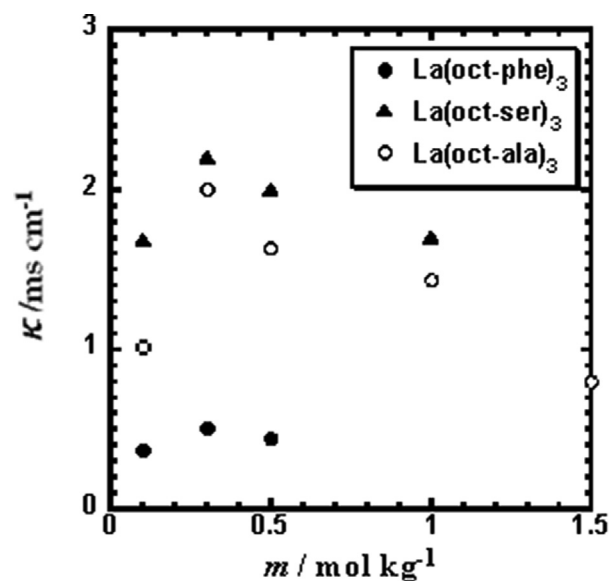
Solvent	La(oct-ala) ₃	La(oct-phe) ₃	La(oct-ser) ₃
Water	3	3	3
Methanol	1	1	1
Ethanol	1	1	1
Cyclohexanol	1	1	3
Hexanol	1	1	3
Dichloromethane	1	1	3
THF	1	1	3
Ethylacetate	2	2	3
Cloroform	1	1	3
Diethylether	3	3	3
Benzene	2	2	3
Dioxane	2	1	3
Cyclohexane	3	3	3

1: >10%, 2: 0.1–10%, 3: <0.1%.

more than 30 mL, it is considered that the solubility is less than 0.1%. As shown in Table 2, the solubility of La(octnt)₃ of the metal soap complex is very low and almost insoluble in the solvents listed. The presence of amino acid polar groups La(oct-ala)₃ and La(oct-phe)₃ makes the solubility in pure solvents higher. La(octnt)₃ was almost insoluble in all the solvents tested in this study. These results in Table 2 show that the solubilities of the acyl-alaninates are remarkably higher than those of the carboxylates. The low solubility in water and organic solvents leads to the limitation of the application of amphoteric metal soap such as La(octnt)₃. Therefore, there is an urgent need of developing the organic rare-earth complexes with good solubility in water and organic solvents (Li et al., 2016; Iida et al., 2006; Naren et al., 2008; Naren et al., 2009; Gerile et al., 2015).

3.3. ¹³C NMR spectra of the rare earth complexes in methanol solutions

The purity of the lanthanum complexes were studied by elemental analysis using ¹³C NMR and moisture tests. Table 3

**Fig.2** Electric conductivities (K) of La(oct-ala)₃, La(oct-phe)₃, and La(oct-ser)₃ in methanol as a function of the concentration (m) of the complex.

shows the ¹³C NMR chemical shift results of the ligand and lanthanum complexes in methanol from 0 to 200 ppm. The NMR results of the lanthanum complex show eleven different ¹³C chemical shifts, which correspond to eleven different functional groups. The NMR spectrum of La(oct-phe)₃ complex shows 15 resonance peaks since it contains a benzene ring. Furthermore, the ¹³C NMR spectra of the ligands and complexes can be used to determine the purity of the rare earth complexes and to further determine the chemical structure of lanthanum complexes.

3.4. The dissociation of metal complexes in solution

The degree of convergence of the metal complexes in the methanol solution was obtained by measuring the self-diffusion coefficient of the lanthanum complexes. The decrease

Table 3 Chemical shifts of the ¹³C NMR spectra of the rare earth complexes in the methanol solution and the corresponding chemical attribution.

Peak Sequence	Functional Group	Chemical Shift ((δ)/ppm)					
		H(oct-ala)	La(oct-ala) ₃	H(ser-ala)	La(ser-ala) ₃	H(oct-phe)	La(oct-phe) ₃
C-1	—COO—	175.51	182.3	175.828	180.1	175.7	182.3
C-2	—CH—	48.88	51.7	62.535	63.2	54.8	57.6
C-3	—CH ₃ , —CH ₂ —OH*	17.375	17.0	55.657	56.6	38.0	39.1
C-4	—C=O, —C ₆ H ₆ *	175.42	176.3	173.064	175.6	127.1–137.7	127.6–139.1
C-5	—CH ₂ —, —C=O*	36.355	36.6	36.438	36.6	175.2	176.1
C-6	—CH ₂ —	26.482	26.5	26.375	26.4	36.4	37.2
C-7	—CH ₂ —	29.79	29.8	29.65	29.8	26.4	27.3
C-8	—CH ₂ —	29.724	30.0	29.724	30.0	29.4	30.6
C-9	—CH ₂ —	32.447	32.5	36.438	32.4	29.5	30.4
C-10	—CH ₂ —	23.257	23.3	23.183	23.2	32.2	34.2
C-11	—CH ₃ , —CH ₂ * —CH ₃ *	14.1	14.1	14.1	14.1	23.1	24.1
C-12	—CH ₃ *	—	—	—	—	14.1	14.1

in the solute self-diffusion coefficient indicates the interaction between solute and solute. Before discussing the aggregation, we verified the probability of the dissociation of the ligand from the metal complexes in solution at lower concentration ranges. Fig. 2 shows the conductivity of three lanthanum complexes, $\text{La}(\text{oct-ser})_3$, $\text{La}(\text{oct-ala})_3$, and $\text{La}(\text{oct-phe})_3$, in methanol as a function of the concentration (Mass molar concentration, Abbreviated as m) of the complex. The magnitude of the conductivity of the lanthanum complexes is in the order of $\text{La}(\text{oct-ser})_3 > \text{La}(\text{oct-ala})_3 > \text{La}(\text{oct-phe})_3$. As the concentration increases to about 0.1–0.3 mol/kg, the conductivities of all three La complex solutions increase indicating that dissociation occurs in the complex solutions. When the concentrations are higher than 0.3 mol/kg, as the molar concentration of mass increases, the conductivities of the complexes solution start to decrease. This is due to the aggregation behavior of metal ions and ligand ions in the solution the formation of aggregate state.

3.5. Self-assemblies of the metal complexes in solutions studied by ^1H NMR self-diffusion

^1H NMR self-diffusion coefficient measurements provides powerful information in monitoring the degree of aggregation in solutions (Hua et al., 2003; Iida et al., 2004; McKale et al., 1988; Iida et al., 1996; Kawabe et al., 2008). In this study, self-diffusion coefficients of the La complexes of oct-ala, oct-phe, and oct-ser, which were used to study the degree of aggregation of the metal complex in methanol, were obtained using ^1H NMR self-diffusion. The decrease in the solute self-diffusion coefficient indicates the interaction between solute and solute.

Fig. 3 shows the self-diffusion coefficient D versus the molar concentration of the complex. The results show that the self-diffusion coefficients of lanthanum complexes decrease as the molar concentrations of the complexes increase. There is a turning point for the $\text{La}(\text{oct-ala})_3/\text{CH}_3\text{OH}$ solution at the rare earth complex concentration of about 0.4 mol/kg. The turning point was observed by vapor pressure results measured at the same concentrations of the complexes studied. This turning point is at the critical concentrations of dissociation/aggregation of the lanthanum complexes in methanol indicating the beginning of the aggregation. As shown in Fig. 2, the turning point for $\text{La}(\text{oct-ser})_3$ complex is near a concentration of 0.15 mol/kg, the $\text{La}(\text{oct-phe})_3$ complex near 0.2 mol/kg, and the turning point of the $\text{La}(\text{oct-ala})_3$ complex is also near 0.2 mol/kg. The turning points of $\text{La}(\text{oct-ser})_3$ and $\text{La}(\text{oct-phe})_3$ complex in methanol are similar. In general, when the aggregation of the surfactant molecules in the solution gradually increases, the movement of the particles in the solution is hindered, and the diffusion coefficient is reduced (Naren et al., 2008; Naren et al., 2009). In addition, with the continuous evaporation of the mixed solvent, the complex aggregates shrink gradually, and aggregates of different sizes are formed. With further heating and cooling after the aggregation, glassy complexes can be obtained.

It is possible to estimate the molecular size (stalk radius) of free solute in methanol using the diffusion coefficient in a methanol solution. With the estimation of the size of the metal complex using the Stokes - Einstein equation, the diffusion coefficient (D) obtained at a low concentration range can be

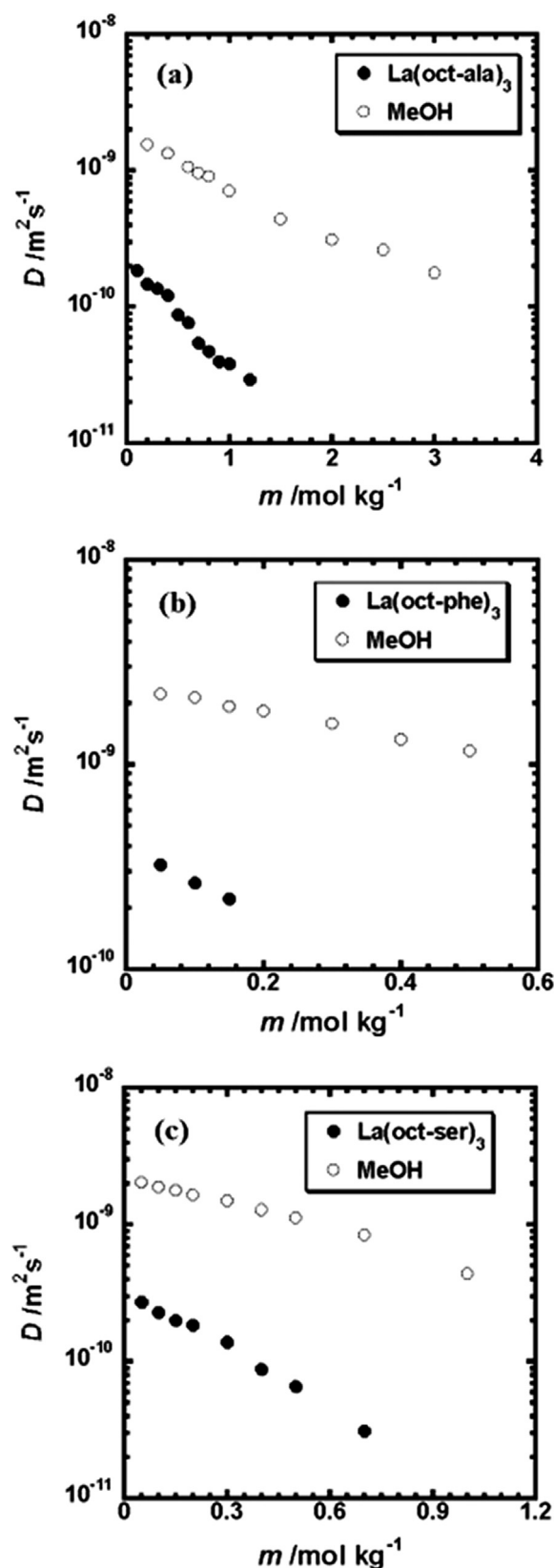


Fig. 3 Plots of the Diffusion coefficient of the lanthanum complexes as a function of solute concentration at 25 ± 1 °C (a) $\text{La}(\text{oct-ala})_3$ in methanol, (b) $\text{La}(\text{oct-phe})_3$ in methanol, (c) $\text{La}(\text{oct-ser})_3$ in methanol.

used directly (Demus et al., 1998). The self-assembly of the Lanthanum(III) complexes at high concentrations was reported as the onset of the formation of the glassy state by solvent-cast method (Naren et al., 2008). There is a trend that the Lanthanum(III) complexes having lower critical concentrations to form aggregations in solutions tend to form more anisotropic assemblies in the solids than those having higher critical concentrations, for example $\text{La}(\text{oct-ala})_3$. At a temperature of 25 ± 1 °C, considering the dissociation of the coordination part of the metal complex, the Stokes radius of $\text{La}(\text{oct-ala})_3$ is calculated in a concentration range of 0.2–0.5 mol/kg, while the Stokes radii of $\text{La}(\text{oct-phe})_3$ and $\text{La}(\text{oct-ser})_3$ are calculated in a concentration range of 0.1–0.2 mol/kg. At 25 ± 1 °C, when $\eta = 0.57$ MPa of the heavy methanol is used (Badawi et al., 2007), the estimated Stokes radius of the complexes studied are as follows. The order of the magnitude of the Stokes radii of the metal complexes in the infinite dilution solution is: $\text{La}(\text{oct-phe})_3 < \text{La}(\text{oct-ser})_3 < \text{La}(\text{oct-oct})_3$, with values of 1.0 nm, 1.3 nm and 2.0 nm, respectively. Small differences in polar groups of the complexes results in small differences in their diffusion coefficient (Stokes radius).

3.6. Dissociation of metal complexes in methanol and the observed vapor pressure drop

The La complexes were found to form aggregates in methanol deduced from the self-diffusion coefficient change. In order to determine the aggregation number of aggregates of these complexes in the solution, the vapor pressure drop of methanol was examined using the reported method (Naren et al., 2009). Fig. 4 shows the results of the vapor pressure drop of $\text{La}(\text{oct-ala})_3$, $\text{La}(\text{oct-phe})_3$, and $\text{La}(\text{oct-ser})_3$ in methanol. The results were calculated using the apparent molecular weight method (Iida et al., 2002; Sato and Watanabe, 2010), where the dissociation of complex ligands in methanol and other solutions was assumed to be minimal. The vapor pressure depression (ΔP) is proportional to the temperature difference (ΔT) between the solvent-wetted thermistor and the solution-wetted one, where ΔT was directly detected (Demus et al., 1998). The aggregation number of associations was determined from the following equation.

$$N = M/M_w = k_{std}/(k_{pn}/M_w)$$

where M is the apparent molecular weight [g mol^{-1}] of the aggregate, M_w is the complex molecular weight [g mol^{-1}] of the monomer, and k_{pn} [$\text{Kg}^{-1} \text{g}$] is the gradient of ΔT . k_{std} is a constant depending on the solvent and apparatus used. The concentration at which the aggregates were observed was similar to the concentration at the turning point of the self-diffusion coefficient. The aggregation number of associations were calculated from the results using benzyl solutions for calibration. Fig. 4 shows the vapor pressure depression versus the concentration of the metal complex in methanol. The results show that there is a turning point for $\text{La}(\text{oct-ala})_3$ at a concentration of 0.4 mol/kg (Fig. 4(a)). When the concentration is lower than 0.4 mol/kg, the aggregation number of $\text{La}(\text{oct-ala})_3$ calculated is 0.9, and the aggregation number of $\text{La}(\text{oct-ala})_3$ is 2.6, when the concentration equals to and greater than 0.4 mol/kg. For $\text{La}(\text{oct-phe})_3$, the turning point

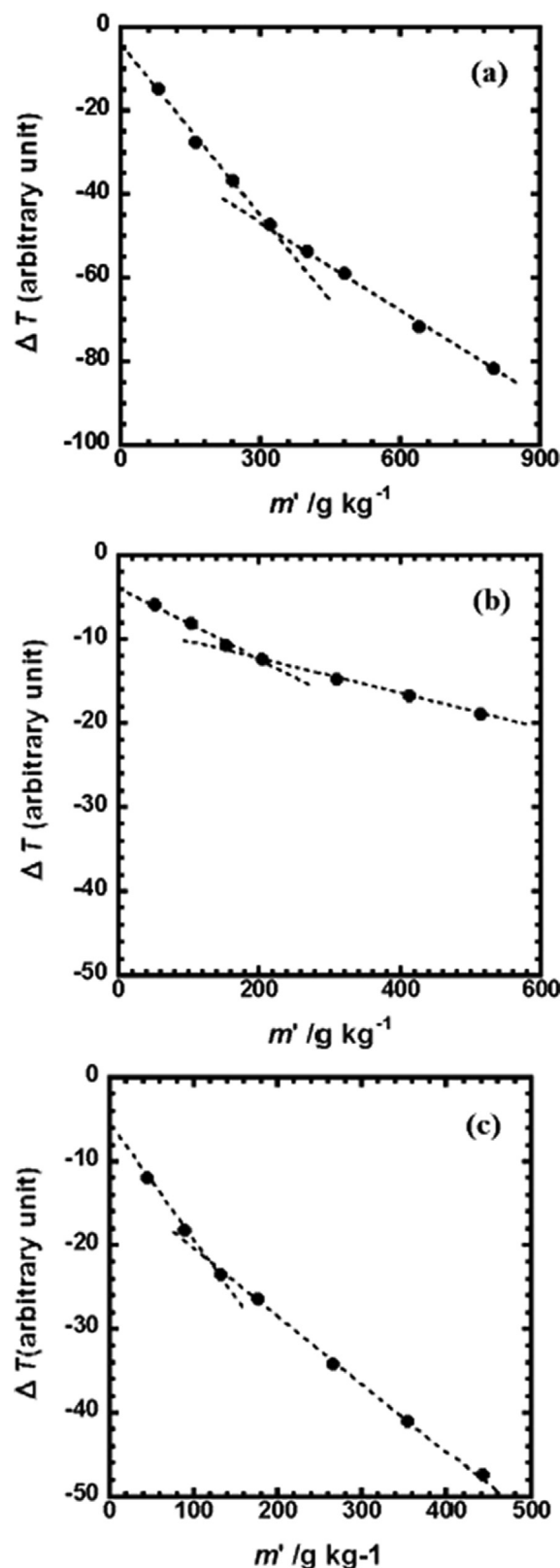


Fig. 4 Vapor pressure depression ($\propto \Delta T$) of (a) $\text{La}(\text{oct-ala})_3 \cdot \text{H}_2\text{O}$ methanol, (b) $\text{La}(\text{oct-phe})_3 \cdot 1.5 \text{H}_2\text{O}$ methanol, and (c) $\text{La}(\text{oct-ser})_3 \cdot 3\text{H}_2\text{O}$ methanol as a function of the concentration of the metal complex (g/kg).

appeared at a concentration of 0.2 mol/kg (Fig. 4(b)). When the concentration is less than 0.2 mol/kg, the aggregation number of $\text{La}(\text{oct-phe})_3$ calculated is 5, and the aggregation number of $\text{La}(\text{oct-phe})_3$ is 9, when the concentration is equal to and greater than 0.2 mol/kg. For $\text{La}(\text{ser-ala})_3$, the turning point presents at a concentration of 0.15 mol/kg (Fig. 4 (c)). When the concentration is smaller than 0.15 mol/kg, the aggregation number of $\text{La}(\text{ser-ala})_3$ calculated is 2.5, and the aggregation number of $\text{La}(\text{ser-ala})_3$ is 3.5, when the concentration is equal to or larger than 0.15 mol/kg. These complexes begin to aggregate at very low concentrations. Here, using the absolute value of the slope k_{p1} of ΔT , $k_{p1} > k_{p2}$ was obtained for the La complexes. In addition, for the order of aggregation numbers, $\text{La}(\text{oct-ala})_3 < \text{La}(\text{oct-ser})_3 < \text{La}(\text{oct-phe})_3$, which was obtained by the diffusion coefficients and by comparing the association concentration of the La complexes in methanol. It is easy for the complex molecules to associate due to the stacking effect of the phenyl groups on the side chains of the amino acids. The hydrogen bond formation of the hydroxyl group significantly affects the association of the complex in methanol.

In principle, as long as the nature of the solution changes with the generation of micelles in the solution, there is a turning point with the concentration curve, the concentration of which is the critical micelle concentration (CMC), so that the critical micelle concentration is obtained by plotting. CMC can be used as a measure of the surface activity of surfactants. The smaller the CMC, the lower the concentration required to form micelles by this active agent, and the lower the concentration at which surface adsorption is saturated. When the concentration of the complex solution is lower than the critical micelle concentration, the dissociation of the complex occurs in solution. When the concentration of the complex solution is greater than the CMC, the dissociation of the ligand ions and metal ions occur in association, and micelles form. When the concentration gradually increases to a certain number, many surfactant molecules immediately combine into large groups to form "micelles", and the movement of particles in the solution is hindered so that the diffusion coefficient of the substance is reduced (Iida et al., 1996; Ishii, 1994). In the non-aqueous system, the adsorption of water increases, and the surfactant in the solution only shows high-level rendezvous behavior (the formation of reverse micelles). In addition, with continuous evaporation of the mixed solvent, the complex aggregates gradually shrink, and different sized aggregates form. Further heating and cooling can form glass state, liquid crystal state, and other rare earth complexes.

3.7. The aggregation of metal complexes in chloroform

The aggregation of the metal complexes formed by hydrophobic interaction is the result of the interactions between the solute and the solvent and the solvent and the solvent. As shown in Fig. 4, for the complexes in methanol, aggregations occur at high concentrations. However, for metal complexes in chloroform, aggregations occur at low concentrations. The results of the ^{13}C NMR, diffusion coefficients, and vapor pressure measurements for the metal complex chloroform solutions show that no peak was observed in the self-diffusion experiment of the heavy d-CDCl_3 solution of the $\text{La}(\text{oct-ala})_3$ complex. The ^{13}C NMR spectrum of the $\text{La}(\text{oct-ala})_3$

complex in chloroform and the full width at half maximum of the peak were obtained. The increase in the concentration of the complex results in a significant increase in the full width at half maximum.(Table 4).

In addition, for the diffusion (Fig. 5) and vapor pressure measurements (Fig. 6) in the vicinity of 0.25 mol/kg, the aggregation number of $\text{La}(\text{oct-ala})_3$ is 11 when the concentration is equal to or greater than 0.25 mol/kg. The transition curve of the diffusion coefficient of the Lanthanum complex in chloroform as a function of the solute concentration shows a turning point at a low concentration of about 0.25 mol/kg, indicating that the Lanthanum complex in chloroform starts to form aggregates at a low concentration.

3.8. Polarized microscopic observation of lanthanum complexes

Fig. 7 shows the surface morphology of the crystal state of Lanthanum Complex by polarizing microscope. It can be seen that crystalline (Fig. 7 (a), (c)) and liquid crystalline.1 (Fig. 7 (d), (e)) showing a colorful color, opaque. The glassy material (Fig. 7(b)) has uniformity, strong transparency and no color, which is almost close to the inorganic glass morphology. Through the observation of the surface morphology of the complex, we can obtain the information on the crystal state and the glass state structure.

3.9. DSC and TG-DTA studies of the various structure states of Lanthanum complexes

In order to determine the glass transition point, melting point, melting enthalpy and the melting point, the DSC experiments were carried out. The DSC curves are shown in Fig. 8. The glass state solid of monohydrate $\text{La}(\text{oct-ala})_3$ complex showed a glass transition point at 70 °C, with two sharp endothermic peaks appearing in the crystalline solid. The same $\text{La}(\text{oct-ala})_3$ crystalline state and the $\text{La}(\text{oct-phe})_3 \cdot 1.5\text{H}_2\text{O}$ complex isolated from the methanol solution also showed two sharp peaks. The optical anisotropy of the $\text{La}(\text{oct-phe})_3 \cdot 1.5\text{H}_2\text{O}$ complex obtained by the different purification and separation methods showed a glass transition point at around 60 °C. The melting enthalpy of this complex is very small ($\Delta H(\text{La}(\text{oct-phe})_3 \cdot 1.5\text{H}_2\text{O}) \approx 7.68 \text{ kJ mol}^{-1}$), being decomposed when heated to above 220 °C. The other symplectic acyl amino acid compound is decomposed at above 250 °C. The optical anisotropy of the $\text{La}(\text{oct-ser})_3 \cdot 3\text{H}_2\text{O}$ complex obtained by the different purification and separation methods showed a glass transition point at around 70 °C, with the complex heated up to be more than 198 °C to lose $3\text{H}_2\text{O}$.

By comparing the melting enthalpy change of complexes with different polar groups, $\Delta H_m(\text{La}(\text{oct-ala})_3 \cdot \text{H}_2\text{O} \text{ crystalline}) (\approx 13 + 94 \text{ kJ mol}^{-1}) > \Delta H_m(\text{La}(\text{oct-phe})_3 \cdot 1.5\text{H}_2\text{O} \text{ crystalline}) (\approx 52.05 + 15.45 \text{ kJ mol}^{-1}) > \Delta H_m(\text{La}(\text{oct-phe})_3 \cdot 1.5\text{H}_2\text{O} \text{ liquid crystalline}) (\approx 7.68 \text{ kJ mol}^{-1})$, separately described low temperature enthalpy change values and high temperature enthalpy change values. The melting enthalpy values reflect the degree of crystallization of the solids.

Fig. 9 presents the TG-DTA curve of lanthanum complexes, among which TGA is the curve of thermal gravimetric analysis, and DTA the endothermic curve of the complex. Fig. 9 shows that the TGA curve of the Lanthanum complex has a significant weight loss step, and that the weight loss

Table 4 The ^{13}C NMR spectrum results of the $\text{La}(\text{oct-ala})_3$ complex in chloroform showing the full widths at half maximum of the observed peaks at various concentrations of the complex.

m (mol/kg)	14.5 ppm (C-11)	22.65 ppm (C-10)	29.25 ppm (C-7, C-8)	31.75 ppm (C-9)
0.05	58.10	48.40	91.90	67.70
0.10	71.50	76.60	127.70	95.70
0.2	76.40	89.10	159.10	101.80
0.3	96.60	158.60	248.30	169.20
0.4	142.90	210.10	362.00	250.00

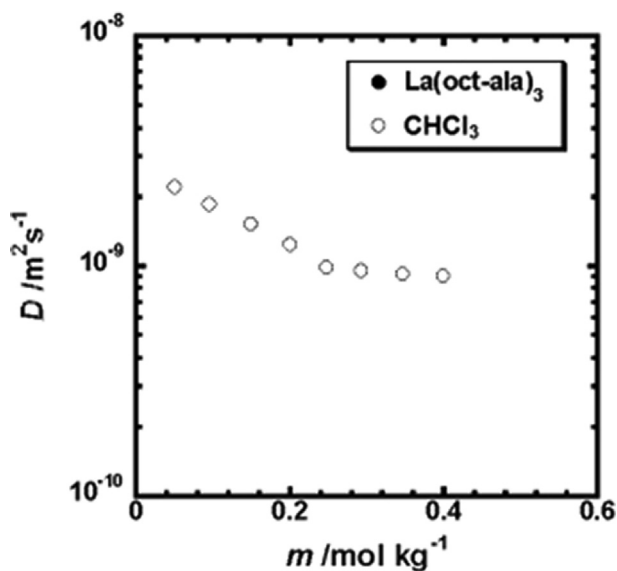


Fig. 5 Plot of the diffusion coefficient of $\text{La}(\text{oct-ala})_3$ in chloroform as a function of solute concentration.

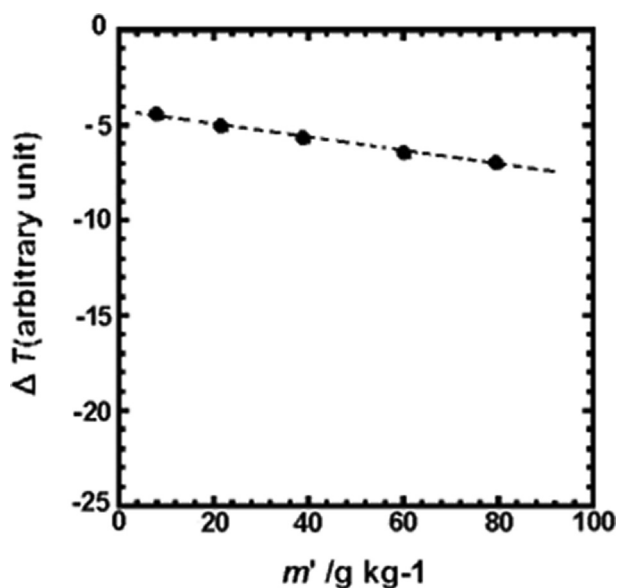


Fig. 6 Vapor pressure depression ($\propto \Delta T$) of (a) $\text{La}(\text{oct-ala})_3 \cdot \text{H}_2\text{O}$ in chloroform as a function of the concentrations (g/kg) of the metal complex.

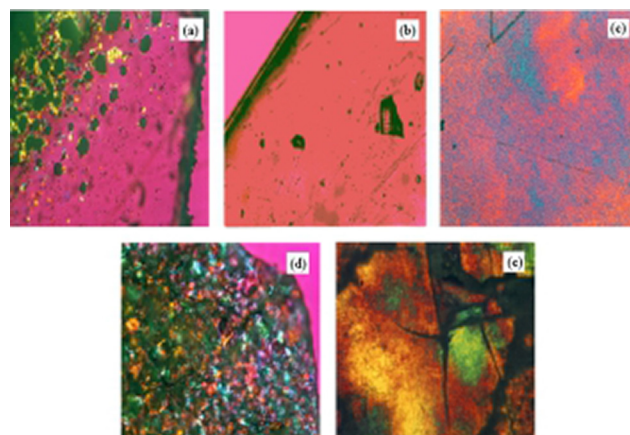


Fig.7 Optical textures observed patterns of complex (a) crystalline $\text{La}(\text{oct-ala})_3 \cdot \text{H}_2\text{O}$; (b) glassy $\text{La}(\text{oct-ala})_3 \cdot \text{H}_2\text{O}$; (c) crystalline $\text{La}(\text{oct-phe})_3 \cdot 1.5\text{H}_2\text{O}$; (d) liquid crystalline $\text{La}(\text{oct-phe})_3 \cdot 1.5\text{H}_2\text{O}$; (e) liquid crystalline $\text{La}(\text{oct-ser})_3 \cdot 3\text{H}_2\text{O}$.

can determine the molar mass of the complex lost water. The decrease corresponds to 1.0, 1.5 and 3 mol water per mol of the metal complex for the 1.0, 1.5 and 3 hydrate complexes, respectively.

3.10. WAXD and SAXS profiles for the solid state

Fig. 10 shows WAXD patterns of crystalline, glassy state and liquid crystalline lanthanum complexes in the test range of $2\theta = 0-60^\circ$. **Fig. 10(a)** and **(b)** is for the $\text{La}(\text{oct-ala})_3$ diffraction pattern, **(c)** and **(d)** is $\text{La}(\text{oct-phe})_3$ diffraction pattern, and **(e)** is $\text{La}(\text{oct-ser})_3$ diffraction pattern. The glassy $\text{La}(\text{oct-ala})_3$, liquid crystalline $\text{La}(\text{oct-phe})_3$, and liquid crystalline $\text{La}(\text{oct-ser})_3$ complexes containing 1, 1.5 and 3 water molecule display broad amorphous diffraction peaks and complexes comprising crystalline $\text{La}(\text{oct-ala})_3 \cdot \text{H}_2\text{O}$ and crystalline $\text{La}(\text{oct-phe})_3 \cdot 1.5\text{H}_2\text{O}$ molecules demonstrate sharp crystalline diffraction peaks. The flattest baseline and the highest peak are seen in the crystalline $\text{La}(\text{oct-ala})_3 \cdot \text{H}_2\text{O}$ and crystalline $\text{La}(\text{oct-phe})_3 \cdot 1.5\text{H}_2\text{O}$ complex. On the other hand, for the glassy $\text{La}(\text{oct-ala})_3$, liquid crystalline $\text{La}(\text{oct-phe})_3$ and liquid crystalline $\text{La}(\text{oct-ser})_3$ complex, the baseline is wavy to the largest extent and the peak intensity is the lowest. A comparison of three complexes shows that $\text{La}(\text{oct-ala})_3$ and $\text{La}(\text{oct-phe})_3 \cdot 1.5\text{H}_2\text{O}$ complexes have a trend to be easily crystallized, and that $\text{La}(\text{oct-ser})_3$ complexes tend to vitrify easily. The

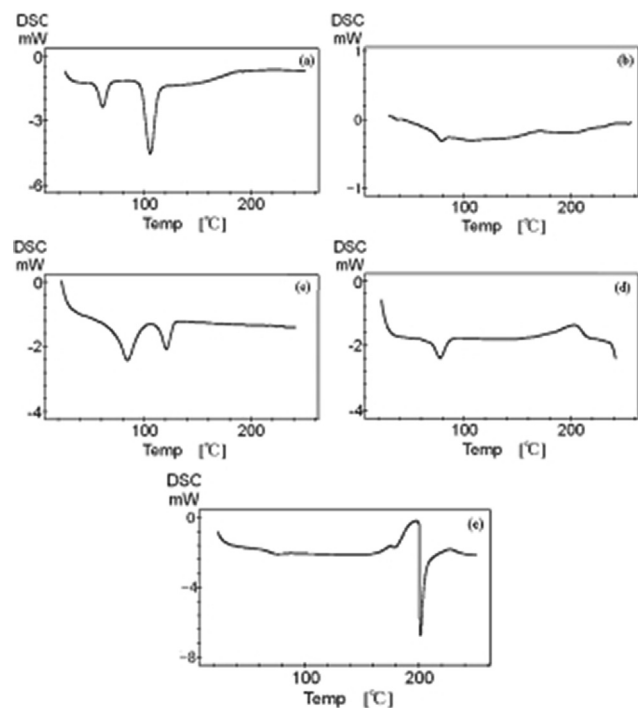


Fig. 8 Temperature dependence of the heat flow during DSC experiment of (a) the complex crystalline $\text{La}(\text{oct-ala})_3 \cdot \text{H}_2\text{O}$, (b) glassy $\text{La}(\text{oct-ala})_3 \cdot \text{H}_2\text{O}$, (c) crystalline $\text{La}(\text{oct-phe})_3 \cdot 1.5\text{H}_2\text{O}$, (d) liquid crystalline $\text{La}(\text{oct-phe})_3 \cdot 1.5\text{H}_2\text{O}$, (e) liquid crystalline $\text{La}(\text{oct-ser})_3 \cdot 3\text{H}_2\text{O}$.

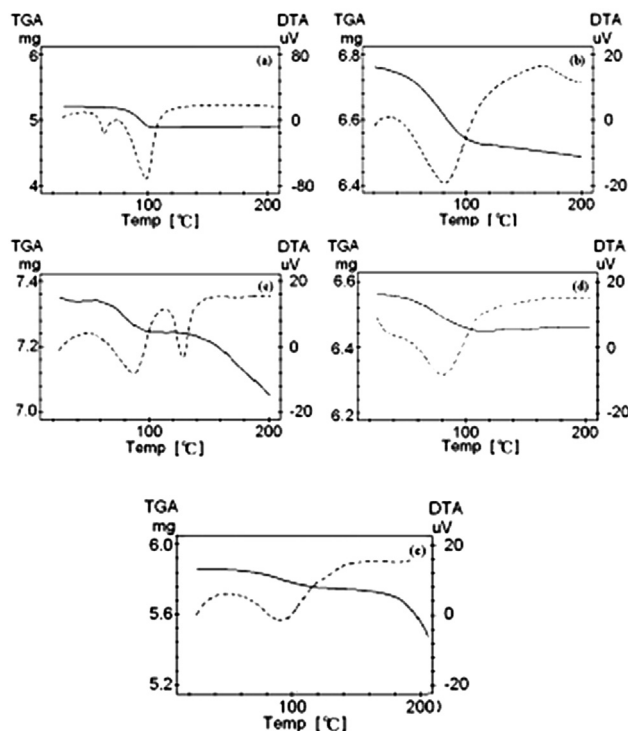


Fig. 9 TG-DTA measurements of the complex (a) crystalline $\text{La}(\text{oct-ala})_3 \cdot \text{H}_2\text{O}$, (b) glassy $\text{La}(\text{oct-ala})_3 \cdot \text{H}_2\text{O}$, (c) crystalline $\text{La}(\text{oct-phe})_3 \cdot 1.5\text{H}_2\text{O}$, (d) liquid crystalline $\text{La}(\text{oct-phe})_3 \cdot 1.5\text{H}_2\text{O}$, (e) liquid crystalline $\text{La}(\text{oct-ser})_3 \cdot 3\text{H}_2\text{O}$.

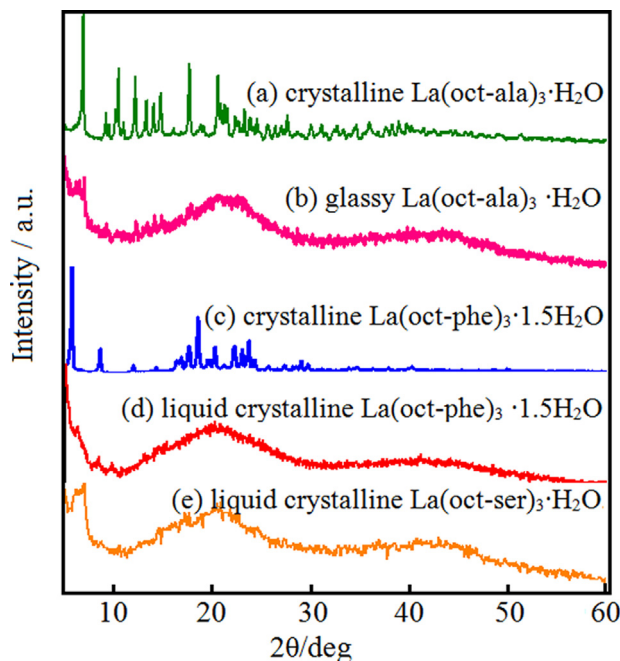


Fig. 10 WAXD patterns of lanthanum complex.

broad scattering curve appearing at around $2\theta = 23\text{--}26^\circ$ originates from the methylene-methylene entanglement interaction and indicates the loss of in-plane ordering, i.e. disordered alkyl-chains. These profiles are independent of the method for the formation of the glassy state (precipitation from solution or annealing treatment) and liquid crystalline, but depend on the Polar functional groups of ligands.

The 1 water molecule glasses $\text{La}(\text{oct-ala})_3 \cdot \text{H}_2\text{O}$, 3 water molecule liquid crystal glass $\text{La}(\text{oct-ser})_3 \cdot 3\text{H}_2\text{O}$ and 1.5 water molecule $\text{La}(\text{oct-phe})_3 \cdot 1.5\text{H}_2\text{O}$ complexes have broad amorphous diffraction peaks. The complexes containing 1 water molecules crystalline $\text{La}(\text{oct-ala})_3 \cdot \text{H}_2\text{O}$ and 1.5 water molecule crystalline $\text{La}(\text{oct-phe})_3 \cdot 1.5\text{H}_2\text{O}$ complex take on sharp crystalline diffraction peaks. Polarizing microscope observation indicates that the unique liquid crystal glass in the glass transition point is near the anisotropic nature. This rare and precious liquid crystal glass is formed by anionic and cationic coulombs acting over very long distances.

The peak half-widths increase in the order of glassy $\text{La}(\text{oct-ala})_3 \cdot \text{H}_2\text{O}$ (peak half-width = 8.4°) (Fig. 11(b)) < liquid crystalline $\text{La}(\text{oct-ser})_3 \cdot 3\text{H}_2\text{O}$ (peak half width = 10°) (Fig. 11(e)) < liquid crystalline $\text{La}(\text{oct-phe})_3 \cdot 1.5\text{H}_2\text{O}$ (peak half width = 10.2°) (Fig. 11(d)). These results indicate the importance of the order and disorder in lanthanum complexes. This order reflects the magnitudes of the disordering of the crystal states, liquid crystal states and glassy states, following the order of the Polar functional groups of ligands. However, there is a direct relationship at the glass transition temperatures and Liquid crystal phase transition temperature (The lower transition temperatures are observed at 75, 60, and 70 °C, for glassy $\text{La}(\text{oct-ala})_3 \cdot \text{H}_2\text{O}$, liquid crystalline $\text{La}(\text{oct-phe})_3 \cdot 1.5\text{H}_2\text{O}$, and liquid crystalline $\text{La}(\text{oct-ser})_3 \cdot 3\text{H}_2\text{O}$ complexes, respectively).

Small angle X-ray scattering (SAXS) experiments were performed to confirm the cyclical nature of the metal complexes.

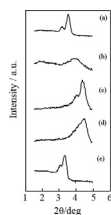


Fig. 11 SAXS profiles for (a) crystalline $\text{La}(\text{oct-ala})_3 \cdot \text{H}_2\text{O}$, (b) glassy $\text{La}(\text{oct-ala})_3 \cdot \text{H}_2\text{O}$, (c) crystalline $\text{La}(\text{oct-phe})_3 \cdot 1.5\text{H}_2\text{O}$, (d) liquid crystalline $\text{La}(\text{oct-phe})_3 \cdot 1.5\text{H}_2\text{O}$, (e) liquid crystalline $\text{La}(\text{oct-ser})_3 \cdot 3\text{H}_2\text{O}$.

The SAXS profile is expected to provide information on supramolecular structures in solid states. Fig. 11 shows the SAXS patterns of crystal state, liquid crystal and glassy state rare earth complexes in the test range of $2\theta = 0^\circ \sim 10^\circ$. From Fig. 11 we can see that crystal and liquid crystal complexes display the sharp Bragg reflection, with the glassy state metal complexes displaying the amorphous diffraction peak width. The SAXS analysis reflects the short range order and disorder characteristics of the rare earth complexes. The extension of the diffraction peak of the glassy state presents that the glassy state is essentially an over cold liquid, and that its structure is characterized by short range order and long range disorder. $\text{La}(\text{oct-ser})_3$ solid has a translucent appearance and demonstrates birefringence. Above T_g , the hard solid gradually changes to a rubberlike material in maintaining anisotropy up to approximately 180 °C. $\text{La}(\text{oct-ser})_3$ complexes present anisotropy in polarized light microscopy, and the disordering in WAXD as well as the ordering in SAXS is characteristic of anisotropic glass and is similar to that observed in liquid crystal. Thus, it was identified that the oct-ser complex assumed an anisotropic glass state, which has been reported in a few cases of metal complexes. We attempted a reduction of water for $\text{La}(\text{oct-ser})_3$ but the trihydrate was unchangeable without decomposition. Larger water content and/or the presence of the hydroxyl group in the serinate complex might have assisted the enhancement of anisotropy for the molecular assembly to form an anisotropic glass.

The XRD determination of the intermediate structure of amino acids metal complexes has been reported by researchers (Nakamura et al., 1992; Tajima et al., 2002). In addition, an empirical equation for evaluating the magnitude of the molecule has been proposed (Marques et al., 1998; Knyazev et al., 2008). Based on these reports, the $\text{La}(\text{oct-ala})_3$ and $\text{La}(\text{oct-phe})_3$ with two layers of crystalline state of the molecular length of 2.5 nm and 2.1 nm from the SAXS test results can be obtained with an increase in the liquid crystal and glass surface d -interval configuration following order: liquid crystalline La

Table 5 The d -spacing estimated from SAXS profiles.

Metal complexes	$2\theta/^\circ$	d/nm
$\text{La}(\text{oct-ala})_3 \cdot \text{H}_2\text{O}$ crystalline	3.38	2.5
$\text{La}(\text{oct-ala})_3 \cdot \text{H}_2\text{O}$ glassy	4.09	2.1
$\text{La}(\text{oct-phe})_3 \cdot 1.5\text{H}_2\text{O}$ crystalline	4.42	2.1
$\text{La}(\text{oct-phe})_3 \cdot 1.5\text{H}_2\text{O}$ liquid crystalline	4.51	2.0
$\text{La}(\text{oct-ser})_3 \cdot 3\text{H}_2\text{O}$ liquid crystalline	3.31	2.7

$(\text{oct-phe})_3 \cdot 1.5\text{H}_2\text{O} <$ glassy $\text{La}(\text{oct-ala})_3 \cdot \text{H}_2\text{O} <$ liquid crystalline $\text{La}(\text{oct-ser})_3 \cdot 3\text{H}_2\text{O}$ (in Table 5).

The above results show that the glass state is formed in a wide range, that the alkyl lock is arbitrarily filled, and that the glass state of d -spacing estimated is shorter than that of the crystalline state. The wide diffraction peak of the glass state indicates the disorder of the molecular structure. The liquid crystal glass state is mainly characterized by the fact that the center of gravity of the molecule is frozen, with the structure of the liquid crystal in order. It is easy for the optical anisotropic glass state to form the same structure as the crystal body complex.

3.11. FT-IR profiles for the solid state

These conformational differences in the alkyl chains between the glassy and the crystalline states were also observed in the methylene stretching mode of the IR spectra in the range 2850–2960 cm^{-1} . In the glass state $\text{La}(\text{oct-ala})_3$ complex, the d -half value width of the peak in this range is significantly larger than those in the crystalline state recorded in Table 6. This broadening arises from the lower ordering of the alkyl chains due to the gauche conformation. A comparison of liquid crystalline $\text{La}(\text{oct-ser})_3$ complexes, crystalline $\text{La}(\text{oct-ala})_3$ and $\text{La}(\text{oct-phe})_3$ complexes of d -half value amplitude indicates that $\text{La}(\text{oct-ser})_3$ half value amplitude variable width, $\text{La}(\text{oct-ser})_3$ Complex d -half value amplitude is 119 cm^{-1} . The FT-IR test results can be obtained from the liquid crystal and glass surface d -interval configuration following the order increase: crystalline $\text{La}(\text{oct-phe})_3 \cdot 1.5\text{H}_2\text{O} <$ crystalline $\text{La}(\text{oct-ala})_3 \cdot \text{H}_2\text{O} <$ liquid crystalline $\text{La}(\text{oct-phe})_3 \cdot 1.5\text{H}_2\text{O} <$ liquid crystalline $\text{La}(\text{oct-ser})_3 \cdot 3\text{H}_2\text{O} <$ glassy $\text{La}(\text{oct-ala})_3 \cdot \text{H}_2\text{O}$. from the above test results it can be seen that the liquid phase material has a unique mesophase property. In addition, this broadening rises from the lower ordering of the alkyl chains due to the gauche conformation.

We attempted to monitor the lanthanide coordination spheres using FT-IR in the range 400–700 cm^{-1} (Bennett et al., 1989; Binnemans et al., 2000; Imura and Suzuki, 1985; Yang et al., 1996). A characteristic peak appears at 550 cm^{-1} , which can be assigned to the lanthanide-O stretching bond. Furthermore, symmetric stretching vibrations of the carboxylate group, ν_{sym} , are detected at 1410 cm^{-1} and the asymmetric stretching vibrations, ν_{asym} at 1550 cm^{-1} , in the present oct-ala complexes. The oct-phe complex is produced in the aromatic C-H stretching absorption band in the range 3100–330 cm^{-1} . The oct-ser complex has an O-H stretching vibration absorption peak in the range of 500–850 cm^{-1} .

Table 6 The IR line widths (cm^{-1}) for the peaks in the range of around 2850–2860 cm^{-1} for the lanthanides complexes in the crystalline and glassy states. The estimation errors are $\pm 4 \text{ cm}^{-1}$.

Metal complexes	Δ/cm^{-1}
$\text{La}(\text{oct-ala})_3 \cdot \text{H}_2\text{O}$ crystalline	83
$\text{La}(\text{oct-ala})_3 \cdot \text{H}_2\text{O}$ glassy	155
$\text{La}(\text{oct-phe})_3 \cdot 1.5\text{H}_2\text{O}$ crystalline	60
$\text{La}(\text{oct-phe})_3 \cdot 1.5\text{H}_2\text{O}$ liquid crystalline	97
$\text{La}(\text{oct-ser})_3 \cdot 3\text{H}_2\text{O}$ liquid crystalline	119

These La complexes are observed at 3400 cm^{-1} near the broad peak of the OH^- stretching vibrational of water molecules, suggesting that complexes are indeed present in water molecules. These DTA-TG analysis results are in agreement; in addition, 500 cm^{-1} in the vicinity of the vibrational peak detection of water molecules are detected, thus determining the La complexes for water molecules to participate in coordination (Imura and Suzuki, 1985; Yang et al., 1996).

3.12. Optical absorption properties

The optical absorption properties of the lanthanum complexes were characterized by UV-Vis absorption spectroscopy. The results are shown in Fig. 12. UV-Vis absorption spectrum measurements of lanthanum complexes were carried out in methanol solution in the range 200–1000 nm. The absorbance of the three lanthanum complexes is zero or less after 400 nm, indicating that the complexes have no optical absorption properties in the visible range. For clarity, Fig. 12 displays the

absorbance only in the range 200–400 nm. For each lanthanum complexes, there ultraviolet absorption peaks can be observed in the range of 200–400 nm. The optical absorption is related to the type of chemical bond. UV-Vis spectrum of $\text{La}(\text{oct-ala})_3$ and $\text{La}(\text{oct-ser})_3$ shows only one band at 216 nm which attributed to $n\text{-}\pi^*$ transition, because they have $\text{C}=\text{O}$ chromophore. But the absorbance of $\text{La}(\text{oct-ser})_3$ is larger than that of $\text{La}(\text{oct-ala})_3$ due to an extra hydroxyl group. The hydroxyl group combines with atoms in the solvent to form hydrogen bond, which can enhance the optical absorbance of the complexes (Seiji and Hirosh, 2014; Iida et al., 1997). UV-Vis spectrum of $\text{La}(\text{oct-phe})_3$ shows two bands at 216 nm and 256 nm which are attributed to $n\text{-}\pi^*$ and $\pi\text{-}\pi^*$ transitions respectively. It not only has a $\text{C}=\text{O}$ chromophore, but also a benzene ring chromophore. For the same complex, the absorbance increases with the concentration of the solution. $\text{La}(\text{oct-phe})_3$ has the best optical absorption performance in solution, and it has a wide ultraviolet absorption range and strong absorbance ($A_{\text{max}} = 3.3$). It can be used as a good optical absorption material.

3.13. EXAFS profiles for the solid state and solution state of the lanthanum complexes

To further obtain the local structure of the rare earth complexes, we studied the microstructure information of the rare earth atoms, the type of interconnecting atoms (La-O), the distance between atoms (r), the inner potential correction ($D E_0$), the Debye-waller factor(s) and coordination numbers (CN) using EXAFS. EXAFS is a powerful technique to determine the local structure of a specific element for non-crystalline system, that is, EXAFS has element selectivity (Yang et al., 1996; Sato and Watanabe, 2010; Ishii, 1994). The coordination state (Rare Earth Ion-O Bonding Coordination) of solid state and concentrated methanol solution of rare earth complexes was studied by EXAFS.

In order to reveal the coordination state around the lanthanide ions clearly, we performed EXAFS experiments for $\text{La}(\text{oct-ala})_3$, $\text{La}(\text{oct-phe})_3$, and $\text{La}(\text{oct-ser})_3$ complexes in both solid and solution states. The least square fitting of atomic spacing, coordination number, etc. of the EXAFS results are shown in Table 7. Table 7 shows that the CN of the oxygen atoms around the lanthanum atom are always maintained as 7.0–7.3 in the $\text{La}(\text{oct-ala})_3$ diversification states (For crystalline, glassy, solution, liquid crystalline, etc.), and as 6.5–7.0 in the $\text{La}(\text{oct-phe})_3$ diversification states, and as 7.0–7.2 in the $\text{La}(\text{oct-ser})_3$ diversification states. The EXAFS results of the lanthanum complexes were compared with the results of the crystalline state of $\text{La}(\text{acac})_3 \cdot 2\text{H}_2\text{O}$. The coordination number of the La-O binding of lanthanum complexes is almost equal to $8(6 + 2)$ for all samples studied. In general, the coordination number (CN) (La-O) of the oxygen atom near the lanthanum atom is considered to be 6, and the coordination number of more than 7 is the result of the coordination of metal ions with water. The coordination number of lanthanum complexes is almost the same in the complex solid and in the solution of the complex.

The above test results can be seen, EXAFS test results provides a rare earth neighbor atoms structure information, And abnormal X-ray scattering provides periodic well ordered and disordered atomic distribution of information.

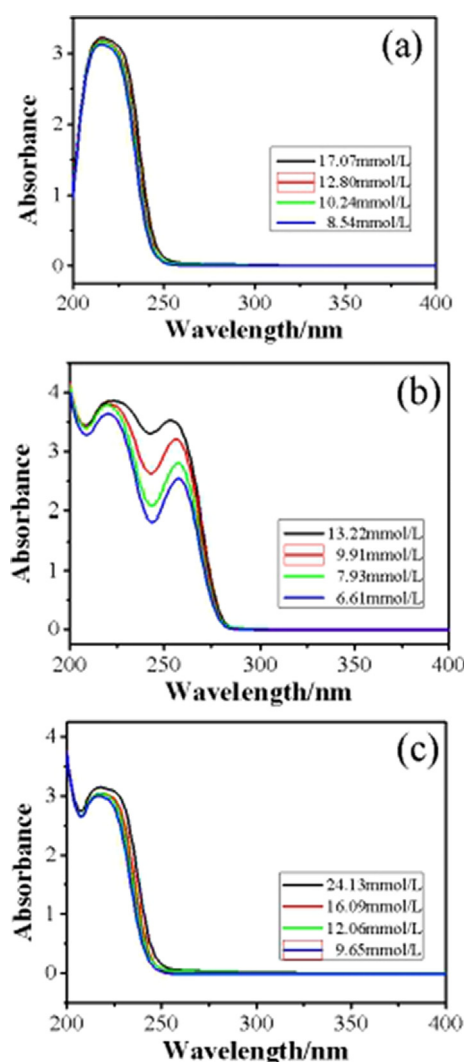


Fig. 12 UV-Vis spectra of (a) $\text{La}(\text{oct-ala})_3$, (b) $\text{La}(\text{oct-phe})_3$, (c) $\text{La}(\text{oct-ser})_3$ complexes in different concentration.

Table 7 Structural parameters from EXAFS analysis of the lanthanum complexes.

Lanthanum Complexes	Bond	CN	r/nm	$\Delta E/eV$	$10^3 \sigma/nm$	R/%
La(acac) ₃ ·2H ₂ O crystalline	La-O	7.8	0.252	15.4	10.9	1.47
La(oct-ala) ₃ ·H ₂ O 1 mol kg ⁻¹ MeOH solution	La-O	7.0	0.255	14.4	10.9	1.23
La(oct-ala) ₃ ·H ₂ O crystalline	La-O	7.2	0.254	14.1	11.1	1.37
La(oct-ala) ₃ ·H ₂ O glassy state	La-O	7.3	0.254	14.3	11.5	1.25
La(oct-phe) ₃ ·1.5H ₂ O 0.5 mol kg ⁻¹ MeOH solution	La-O	6.3	0.249	14.0	11.0	1.03
La(oct-phe) ₃ ·1.5H ₂ O crystalline	La-O	6.5	0.251	14.1	11.1	1.01
La(oct-phe) ₃ ·1.5H ₂ O liquid crystalline	La-O	7.0	0.252	14.2	11.2	0.95
La(oct-ser) ₃ ·3H ₂ O 1 mol kg ⁻¹ MeOH solution	La-O	7.1	0.252	14.0	11.1	1.22
La(oct-ser) ₃ ·3H ₂ O liquid crystalline	La-O	7.2	0.254	14.2	11.2	1.38

The *R* factor is defined as $[k^3(k)_{obs} - k^3(k)_{calc}]^2 / [k^3(k)_{obs}]^2 \cdot 100$. The error bar of *r* and C.N. were estimated by varying the *E* value (± 10 eV) and the values (± 0.01 Å), respectively. The estimated error bars in the C.N. and *r* values are $\pm 10\%$ and ± 0.03 Å, respectively.

4. Conclusion

In summary, new multifunctional amino acid lanthanum surfactant complexes, La(oct-ala)₃, La(ser-oct)₃, and La(oct-phe)₃ were successfully synthesized by the solution chemical method with a product yield of 85% and high purity through the reaction of C₁₁H₂₁NO₃, C₁₁H₂₁NO₄, C₁₇H₂₆NO₃ with LaCl₃, respectively. Structural characteristics of the lanthanum acylaminocarboxylates related to the formation of aggregates were explored by changing the head groups of the ligands. Results show that the effect of different polar ligands on the properties of metal complexes is significant. The presence of amino acids, which contains polar groups, oct-ala and oct-phe, make the solubility of the lanthanum complex higher in pure solvents, but oct-ser complex preferred protic solvents to aprotic solvents. The smaller the critical micelle concentration (CMC) and the lower the concentration required to form micelles by this active agent, and the lower the concentration at which surface adsorption is saturated. When the concentration of the complex solution is lower than the critical micelle concentration, the dissociation of the complex occurs in solution. When the concentration of the complex solution is greater than the CMC, the dissociation of the ligand ions and metal ions occur in association, and micelles form. When the concentration gradually increases to a certain number, many surfactant molecules immediately combine into large groups to form “micelles”, and the movement of particles in the solution is hindered so that the diffusion coefficient of the substance is reduced. In addition, the complex aggregates gradually shrink and different sized aggregates form with continuous evaporation of the mixed solvent. Further heating and cooling lead to form the glass state, liquid crystal state, and crystal state rare earth complexes.

The rare earth amino acid complexes are formed by the combination of nontoxic amino acid ligands with good solubility and rare earth ions can effectively reduce the toxicity of rare earth ions in life body, which can be applied in solar cell devices, polychromatic display, medicine and many other fields.

Acknowledgement

Project supported by the National Natural Science Foundation of China (Grant Nos. 21663018, 51662034), the Natural Science fund Project of Inner Mongolia (Grant Nos. 2018MS02011).

References

Azhar, A., Li, Y.C., Cai, Z.X., Zakaria, M.B., Masud, M.K., Hossain, MdS.A., Kim, J., Zhang, W., Na, J., Yamauchi, Y., Hu, M., 2019.

- Nanoarchitectonics: a new materials horizon for prussian blue and its analogues. *Bull. Chem. Soc. Jpn.* 92 (4), 875.
- Badawi, A.M., Mekawi, M.A., Mohamed, A.S., Mohamed, M.Z., Khowdairy, M.M., 2007. Surface and biological activity of some novel cationic surfactants. *J. Surfactants Deterg.* 10 (4), 243.
- Bennett, A.M.A., Foulds, G.A., Thornton, D.A., 1989. The IR and ¹H, ¹³C NMR spectra of the nickel(II), copper(II) and zinc(II) complexes of 2,4-pentanedione, 4-imino-2-pentanone, 4-thioxo-2-pentanone and 2,4-pentanedithione: a comparative study[J]. *Polyhedron* 18 (8), 2305.
- Binnemans, K., Galyametdinov, Y.G., Deun, R.V., Bruce, D.W., Collinson, S.R., Polishchuk, A.P., Bikchantaev, I., Haase, W., Prosvirin, A.V., Tinchurina, L., Litvinov, I., Gubajdullin, A., Rakhmatullin, A., Uytterhoeven, K., Meervelt, L.V., 2000. Rare-earth-containing magnetic liquid crystals. *J. Am. Chem. Soc.* 122, 4335.
- Demus, D., Goodby, J.W., Gray, G.W., Spiess, H.W., 1998. *Handbook of Liquid Crystals*. V. Vill, Wiley VCH, Weinheim.
- Du, J., Zhang, J., Fang, B., 2003. Properties and applications of amino-acid complex. *Prog. Chem.* 15 (4), 288.
- Gerile, N., Hua, E., Tian, X., 2015. Solubility and aggregation behavior of capryloyl alaninate magnesium(II), calcium(II) and zinc(II) complexes. *Fine Chem.* 32 (7), 741.
- Hua, E., Asaoka, N., Hisamatsu, N., Iida, M., Imae, T., 2003. Effects of metal-counterion interactions on the percolation in microemulsions composed of bis(N-octylethylenediamine)metal(II) complexes in water/benzene and water/chloroform systems. *Colloids Surfaces A Physicochem. Eng. Asp.* 221, 119.
- Hua, E., Ohkawa, S., Iida, M., 2007. Aggregation behavior of alkylethylenediamine palladium(II) complexes in water and in water/organic solvent mixtures. *Colloids Surf A.* 301, 189.
- Hua, E., Izutani, J., Naren, G., Iida, M., 2011. Aggregation of bis (N-octanoylaminocarboxylato) magnesium (II) complexes in water/organic solvents. *Colloids Surfaces A Physicochem. Eng. Asp.* 392 (1), 213.
- Iida, M., 2002. Aggregations of metal complex surfactants in solutions. *Curr. Top Collo. Interf. Sci.* 5, 203.
- Iida, M., Yamamoto, M., Fujita, N., 1996. Multinuclear NMR studies on micellar formation of aqueous [Co (N-octyl-or N-dodecylethylenediamine)(3, 7-Diazanonane-1, 9-diamine)]³⁺ solutions. *Bull. Chem. Soc. Jpn.* 69, 3217.
- Iida, M., Yonezawa, A., Tanaka, J., 1997. A novel reverse micellar system composed of bis(octylethylenediamine)zinc(II) chloride in aqueous benzene and chloroform solutions. *Chem. Lett.* 26 (7), 663.
- Iida, M., Tanase, T., Asaoka, N., Nakanishi, A., 1998. A molecular structure of Bis (N-octylethylenediamine) zinc (II) nitrate in crystal

- and the aggregations in wet chloroform and benzene solutions. *Chem. Lett.* 27 (12), 1275.
- Iida, M., Asayama, K., Ohkawa, S., 2002. The aggregation of dichlorobis (N-hexylethylenediamine) zinc(II) in water and water/chloroform mixed solvents. *Bull. Chem. Soc. Jpn.* 75 (3), 521.
- Iida, M., Masuda, R., Naren, G., Bin, Y.Z., Kajiwara, K., 2004. Formation of stable molecular glasses of yttrium (III) acyl-DL-alaninate complexes. *Chem. Lett.* 33, 1462.
- Iida, M., Inoue, M., Tanase, T., Takeuchi, T., Sugibayashi, M., Ohta, K., 2004. Formation of thermotropic and lyotropic liquid crystals of Bis (N-alkylethylenediamine) silver (I) nitrate. *Eur. J. Inorg. Chem.* 19, 3920.
- Iida, M., Naren, G., Hashimoto, S., 2006. Formation of molecular glasses of (N-acylalaninato) europium (III) complexes and the luminescence properties. *J. Alloy. Compd.* 408, 1022.
- Imura, H., Suzuki, N., 1985. Evaluation of the liquid-liquid partition coefficient of bis (acetylacetonato) copper(II): contribution of specific solute-solvent interaction. *J. Radioanal. Nucl. Ch.* 88 (1), 63.
- Ishii, T., 1994. Principles of the theory of EXAFS. *Toukyou Syoukhou*.
- Jiao, X., Zhang, C., Zhang, H., 2009. Analysis of Surfactants. Chemical Industry Press.
- Kadoda, K., 2006. Function and application of surfactants. *Tokyo C.*
- Kaneti, Y.V., Dutta, S., Hossain, Md.S.A., Shiddiky, M.J.A., Tung, K.L., Shieh, F.K., Tsung, C.K., Wu, K.C.W., Yamauchi, Y., 2017. Strategies for improving the functionality of zeolitic imidazolate frameworks: tailoring nanoarchitectures for functional applications. *Adv. Mater.* 29, 1700213.
- Kawabe, T., Naito, M., Fujiki, M., 2008. Polysilane organogel with hierarchical structures formed by weak intra-/inter-chain Si/FC and van der Waals interactions. *Polym. J.* 40 (4), 317.
- Knyazev, A.A., Galyametdinov, Y.G., Goderis, B., Driesen, K., Goossens, K., Görller-Walrand, C., Binnemans, K., Cardinaels, T., 2008. Liquid-crystalline ternary rare-earth complexes. *Eur. J. Inorg. Chem.* 5, 756.
- Li, Z., Lin, D., Zhang, A., 2016. The progress in research on rare earth pricing. *Chinese Rare Earths* 37 (1), 145.
- Li, Z.M., Liu, Y.L., Sun, J.Y., Zhang, L., Lin, D.L., 2017. Analysis of global rare earth production and consumption structure. *Chinese Rare Earths.* 38 (3), 149.
- Marques, E.F., Burrows, H.D., Miguel, M.G., 1998. The structure and thermal behaviour of some long chain cerium(III) carboxylates. *J. Chem. Soc., Faraday Trans.* 94, 1729.
- McKale, A.G., Veal, B.W., Paulikas, A.P., Chan, S.K., Knapp, G.S., 1988. Improved ab initio calculations of amplitude and phase functions for extended X-ray absorption fine structure spectroscopy. *J. Am. Chem. Soc.* 110, 3763.
- Mizuno, Y., Miyagawa, Y., Kitagawa, Y., Iida, M., Tada, Y., Yokoyama, H., 1998. Effects of tripositive cobalt (III)-complex ions on the structure of a cholesteric mesophase composed of potassium N-dodecanoyl-L-alaninate. *Langmuir* 14, 7058.
- Nakamura, A., Koshinuma, M., Tajima, K., 1992. Solubilization of copper(II) complexes of N-alkyl- β -alanines in their micellar solutions. *Colloids Surf. A* 67 (9), 183.
- Naren, G., Masuda, R., Iida, M., Harada, M., Kurosu, H., Suzuki, T., Kimura, T., 2008. Formation of molecular glasses and the aggregation in solutions for lanthanum (III), calcium (II), and yttrium (III) complexes of octanoyl-DL-alaninate. *Dalt. Trans.*, 1698
- Naren, G., Yasuda, A., Iida, M., Harada, M., Suzuki, T., 2009. Kato K. Aggregation in methanol and formation of molecular glasses for europium(III) N-acylaminocarboxylates: effects of alkyl chain length and head group. *Dalt. Trans.*, 5512
- Naren, G., Zhou, N.B., Tian, X., Bao, F., 2016. Preparation and characterization of capryloyl alanine europium and terbium complexes. *Chinese Rare Earths* 37 (1), 27.
- Perju, E., Cozanc, V., Marin, L., Bruma, M., 2015. Semiflexible thermotropic polyazomethines based on o-dianisidine mesogenic core. *Liq. Cryst.* 42 (9), 1309.
- Sato, S., Watanabe, M., 2010. Introduction to Synchrotron Radiation Research. Shanghai Jiaotong University Press, Shanghai.
- Seiji, U., Hirosh, O., 2014. Structure and Properties of Side Group Thermotropic Liquid Crystal Polymers. Wiley-VCH Verlag GmbH & Co. KGaA.
- Silverstein, R.M., Webster, F.X., Kiemle, D.J., Bryce, D.L., 2014. Spectrometric Identification of Organic Compounds. John Wiley & Sons.
- Szwarc, H., Bessada, C., 1995. Glassy crystals: Correlation between molecular symmetry and glass transition. *Thermochim. Acta* 266, 1.
- Tajima, K., Tsutsui, T., Imai, Y., Nakamura, A., Koshinuma, M., 2002. New phase formation of dimyristoylphosphatidylglycerol bilayer-assembly with sodium or ammonium ions: gelation phenomena in the lamellar liquid crystals aged in water. *Chem. Lett.* 31 (1), 50.
- Tang, J., Salunkhe, R.R., Zhang, H.B., Malgras, V., Ahamad, T., Alshehri, S.M., Kobayashi, N., Tominaka, S., Ide, Y., Kim, J.H., Yamauchi, Y., 2016. Bimetallic metal-organic frameworks for controlled catalytic graphitization of nanoporous carbons. *Sci. Rep.* 6 (1), 651.
- Wang, M., Yu, C.L., He, D.B., Feng, S.Y., Li, S.G., Zhang, L.Y., Zhang, J.J., Hu, L.L., 2011. Enhanced $2\mu\text{m}$ emission of Yb-Ho doped fluorophosphates glass. *J. Non-Crystal. Solids* 2011 (357), 2447.
- Yang, L., Wu, J., Ju, X., 1996. Synthesis, characterization and EXAFS of novel rare earth complexes. *Acta Chim. Sin.* 54, 3.
- Yusuf, V.K., Zhang, J., He, Y.B., Wang, Z.J., Tanaka, S.S.K., Hossain, A.Md.S.A., Pan, Z.Z., Xiang, B., Yang, Q.H., Yamauchi, Y., 2017. Fabrication of an MOF-derived heteroatom-doped Co/CoO/carbon hybrid with superior sodium storage performance for sodium-ion batteries. *J. Mater. Chem. A* 5, 15356.
- Zhang, H., 2017. New uses of rare earth complexes in the field of organic light emitting diodes. In: 9th Natl. Conf. Int. Forum Rare Earth Lumin. Mater(Guangzhou).